Materials Letters 242 (2019) 91–94

Contents lists available at ScienceDirect

Materials Letters

journal homepage: www.elsevier.com/locate/mlblue

A novel approach to achieve high yield strength high nitrogen stainless steel with superior ductility and corrosion resistance

H. Zhang, P. Xue *, D. Wang, L.H. Wu, D.R. Ni, B.L. Xiao *, Z.Y. Ma

Shenyang National Laboratory for Materials Science, Institute of Metal Research, Chinese Academy of Sciences, 72 Wenhua Road, Shenyang 110016, China

ARTICLE INFO

Article history:
Received 2 January 2019
Received in revised form 11 January 2019
Accepted 14 January 2019
Available online 21 January 2019

Keywords:
High nitrogen stainless steel
Friction stir processing
Microstructure
Mechanical properties
Corrosion

ABSTRACT

A complex structure consisting of ultrafine-grained processed zone and coarse-grained base material zone was developed in this study, aiming at improving the yield strength of a high nitrogen stainless steel without sacrificing corrosion resistance and ductility. The ultrafine-grained processed zone was produced by friction stir processing, leading to ultra-high strength and great pitting corrosion resistance, but significantly reduced ductility; the coarse-grained zone exhibited excellent ductility but a very low yield strength. The enhancement and coordination between the processed zone and coarse-grained zone resulted in significantly improved yield strength and ductility of the complex structure. Thus, a combination of excellent mechanical properties and corrosion resistance was successfully achieved.

1. Introduction

With the addition of N, high nitrogen stainless steel (HNS) showed significantly improved pitting corrosion resistance compared to the common 304 stainless steel [1]. However, the relatively low yield strength of the HNS inhibited its wide application.

Traditional methods for increasing the yield strength of the HNS were mainly alloying, cold working and grain refinement [2–4]. However, it should be stressed that obtaining ultra-high N content HNS requires high-cost equipment, and the microstructural control becomes very hard. After cold working, the ductility and corrosion resistance of the HNS decreased sharply due to the high defect density [5,6]. Similarly, the ultrafine-grained microstructure obtained via severe plastic deformation (SPD) also showed inferior ductility [7]. From the results above, it is very clear that traditional processing methods cannot balance mechanical properties and corrosion resistance. Thus, a new method for achieving high yield strength HNS with great ductility and corrosion resistance is highly demanded.

Nowadays, structural design has attracted massive attention [8,9]. With proper design, great combination of strength and ductility [10], significantly improved corrosion resistance [11] and enhanced wear resistance [12] could be achieved. Thus, structural designing could provide a new way of improving the yield strength of the HNS without deteriorating the ductility and corrosion resistance. Friction stir processing (FSP), as a flexible SPD method, is very suitable for microstructure modification and structural design.

In this study, a novel process of tailoring the microstructure of the HNS was developed to construct a complex structure by using FSP. It was shown that an excellent combination of the mechanical properties and corrosion resistance was achieved in such complex structure.

2. Experimental procedures

2 mm thick solid-solution state HNS sheets with a chemical composition of 0.04C-15.81Mn-18.36Cr-2.19Mo-0.66 N-Fe were used as the base material (BM) in this study. Pinless cermet tool with a diameter of 10 mm was used for FSP. The rotation speed of the tool was 300 rpm and the traverse speed was 25 mm/min. Additional flowing water cooling was adopted in order to achieve ultrafine microstructure.

Cross-sectional specimens for optical microscopy observation were polished and electrolytically etched in a 10% oxalic acid solution. Detailed microstructure was investigated via transmission electron microscopy (TEM). Surface morphologies after pitting immersion corrosion tests were examined by scanning electron microscopy (SEM). Vickers hardness and tensile tests were used to evaluate the mechanical properties of the specimens, the gauge length of the tensile specimens was 2.5 mm. For comparative study, the corrosion resistance and mechanical properties of a 2 mm thick 50% cold-rolled HNS were investigated. Detailed experimental information was given in our previous studies [13,14].

* Corresponding author.
E-mail addresses: pxue@imr.ac.cn (P. Xue), blxiao@imr.ac.cn (B.L. Xiao).

https://doi.org/10.1016/j.matlet.2019.01.078
0167-577X/

3. Results and discussion

The cross-sectional morphology of the complex structure after FSP is shown in Fig. 1(a). The complex structure consisted of processed zone (PZ), transient zone and coarse-grained zone. Though no pin was used, a large depth PZ up to ~ 800 μm was obtained. It should be stressed that the depth of the PZ could be designed by using different welding tools and should be controlled based on the thickness of BM.

The grain size of the BM was about 70 μm as shown in Fig. 1(b), and the dislocation density was very low (Fig. 1(c)). After cold rolling, high density of dislocations and twins could be observed (Fig. 1(d)). It should be noted that uniform ultrafine-grained microstructure with a grain size of ~ 400 nm was achieved via FSP (Fig. 1(e)). Due to the dynamic recrystallization, the defect density of the PZ was significantly lower than that of the cold-rolled sample.

After an 8 h immersion corrosion test, the surface morphologies of the various samples are shown in Fig. 2(a). The solid-solution state BM showed high pitting corrosion resistance, only a few small pits with a diameter of ~ 50 μm could be observed. However, the cold-rolled sample showed significantly decreased corrosion resistance, many large pits with a diameter over 100 μm could be well observed, which was consistent with previous study [15]. It should be stressed that the ultrafine-grained surface of the complex structure exposed to corrosion medium showed surprisingly good corrosion resistance, very few pits with a diameter less than 20 μm were observed. As shown in Fig. 2(b), the BM and FSP samples showed significantly higher film breakdown potentials compared to the cold-rolled sample. Obviously, the complex structure showed comparable corrosion resistance to the solid-solution state BM, which should be mainly attributed to the low defect density and uniform ultrafine microstructure.

The results of tensile tests are shown in Fig. 2(c). The BM showed excellent uniform elongation up to ~ 60%, however, the yield strength of the BM was relatively low (~540 MPa). With 50% cold deformation, the yield strength of the HNS was significantly improved (~1300 MPa), nevertheless, the uniform elongation decreased drastically. After FSP, the strength of the PZ was very close to that of the cold-rolled sample, the uniform elongation also decreased significantly. By comparison, the complex structure consisting of the PZ and BM showed significantly improved yield strength (~950 MPa) and good uniform elongation (~30%). It should be noted that, the thickness of the PZ should be carefully controlled. If the PZ is too thin, the improvement of the yield strength would be less effective; if the PZ is too thick, the elongation would drop significantly, and inhomogeneous deformation might occur.

The hardness distribution map of the cross-section is shown in Fig. 2(d). The PZ showed high hardness up to 460 Hv while the hardness of the BM was about 270 Hv. Clearly, the complex structure composed of "hard zone" and "soft zone" exhibited an excellent combination of strength and ductility. From the results above, high pitting corrosion resistance HNS with almost doubled yield strength and high uniform elongation was successfully obtained via structural design.

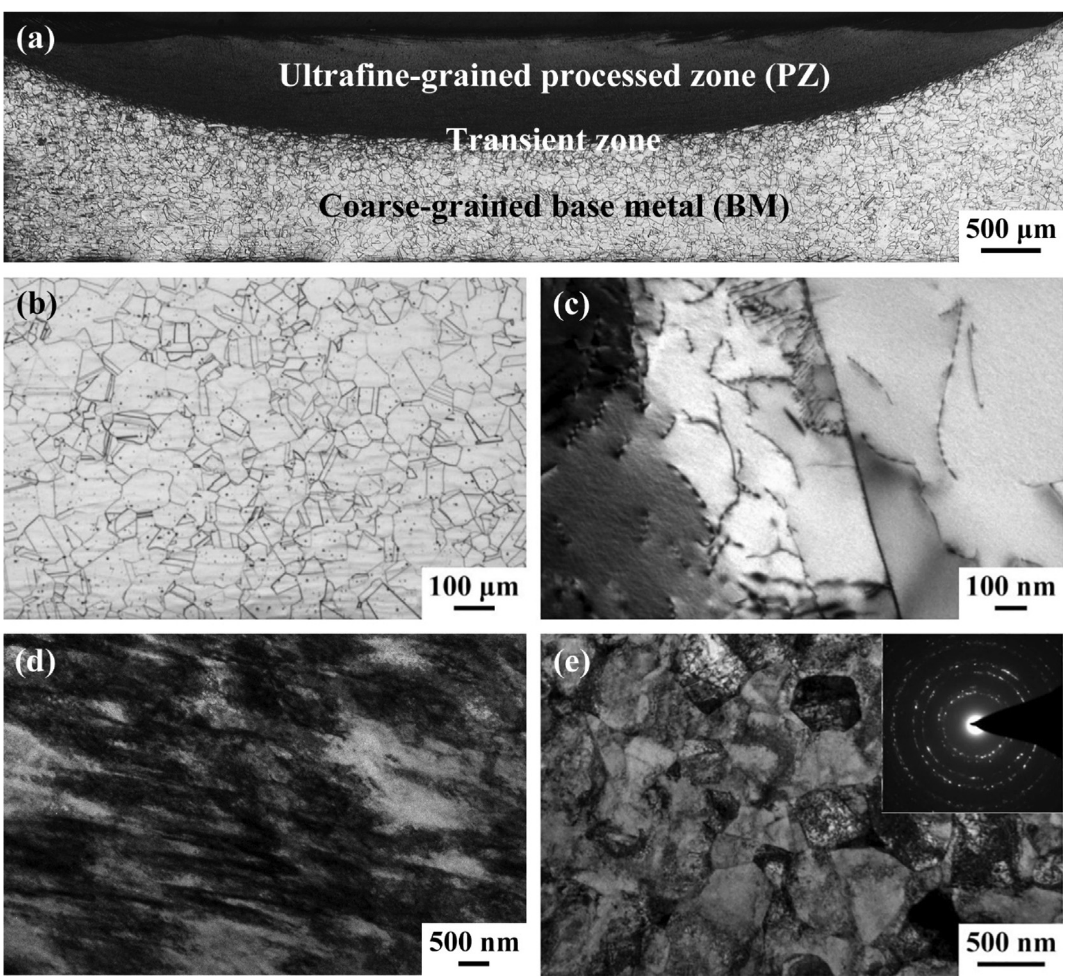

Fig. 1. (a) Macrostructure of complex structure, microstructure of (b, c) BM, (d) cold-rolled HNS, (e) processed zone.

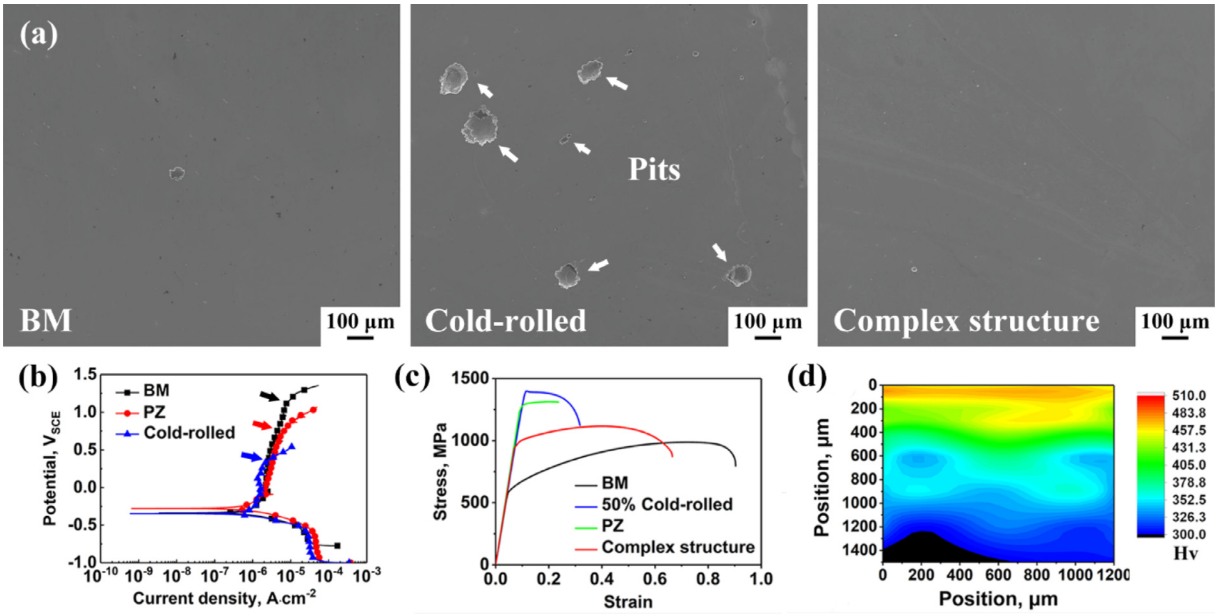

Fig. 2. (a) Surface corrosion morphologies after immersion tests, (b) polarization curves in 3.5% NaCl solution, (c) engineering stress-strain curves, (d) hardness distribution map of complex structure.

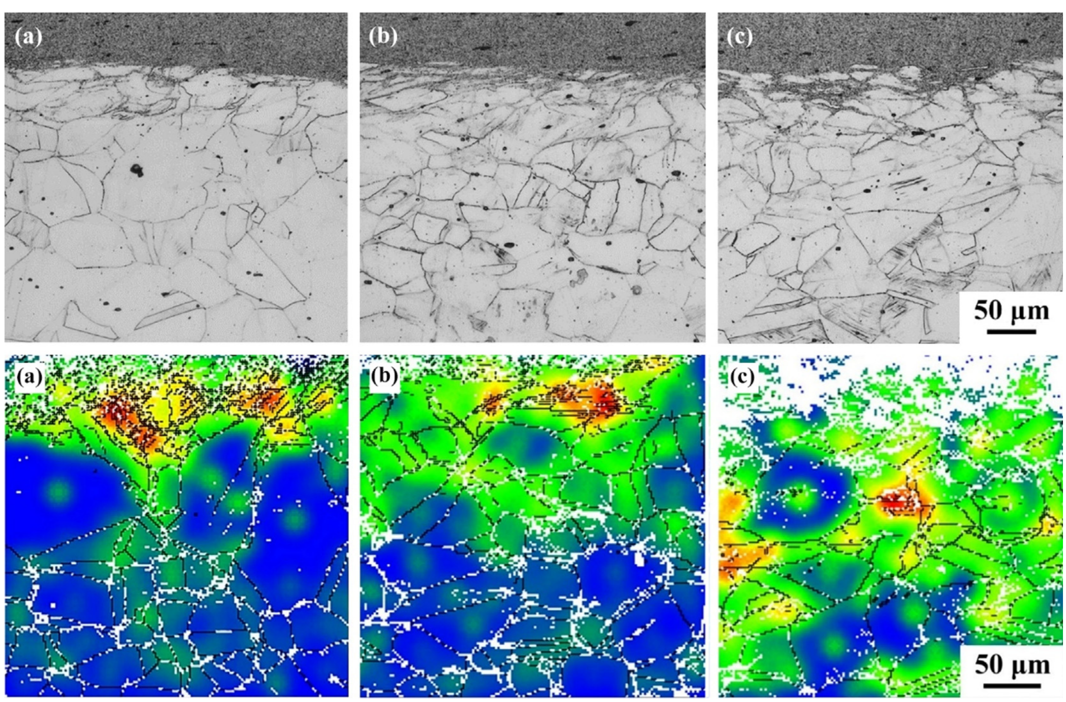

Fig. 3. Microstructure and kernel average misorientation map of the transient zones under (a) 5%, (b) 10%, (c) 20% tensile strain.

Fig. 3 shows the microstructure of the 5%, 10% and 20% deformed tensile specimens. The mixing of fine grains and coarse grains in the transient zone could be observed, which shared some structure characteristics in annealed low-alloyed ferritic steel [16]. The coordination between fine grains and coarse grains could affect strain transferring. From the kernel average misorientation map of the transient zone, it could be clearly observed that the strain was transferred from the transient zone to the coarse-grained zone. It is believed that such strain transfer relieved the strain concentration, thereby resulting in improved uniform elongation.

4. Conclusions

In summary, combining high strength, high corrosion resistance PZ produced by FSP with high ductility coarse-grained BM, a novel high-performance complex structure was developed. Despite the low ductility of the PZ (9%) and inferior yield strength of the BM (∼540 MPa), the combination and coordination of the "hard zone" and "soft zone" resulted in high yield strength (∼950 MPa) and good uniform elongation (∼30%). Furthermore, no significant deterioration in the pitting corrosion resistance was observed in the complex structure. The excellent comprehensive performance should be mainly attributed to the low defect density of the PZ and the alleviation of strain concentration in the transient zone.

Conflict of interest

This article is our original research work and neither this article nor one with substantially similar content under our authorship has been published or is being considered for publication elsewhere. If accepted, the article will not be published elsewhere in the same form, in any language, without the written consent of the publisher. All authors have participated sufficiently in this work to take public responsibility for it, and all authors have reviewed the final version of the manuscript and approved it for publication. No conflict of interest exists.

Acknowledgments

This work was supported by the National Natural Science Foundation of China under grant Nos. 51331008 and 51671190. The authors would like to acknowledge Dr. Q.N. Song (Hohai University) for kindly performing electrochemical tests.

References

[1] J.W. Simmons, Mater. Sci. Eng., A 207 (1996) 159–169, https://doi.org/10.1016/0921-5093(95)09991-3.
[2] H. Bing, Z. Li, Hua Jiang, Z. Rui, Y. Zhang, J. Yang, Iron Steel Res. Int. 16 (2009) 58–61, https://doi.org/10.1016/S1006-706X(09)60011-X.
[3] P. Müllner, C. Solenthaler, P. Uggowitzer, M.O. Speidel, Mater. Sci. Eng., A 164 (1993) 164–169, https://doi.org/10.1016/0921-5093(93)90655-X.
[4] F.Y. Dong, P. Zhang, J.C. Pang, Q.Q. Duan, Y. Bin Ren, K. Yang, Z.F. Zhang, Acta Metall. Sin. (English Lett.) 29 (2016) 140–149, https://doi.org/10.1007/s40195-016-0370-9.
[5] Q. Wang, B. Zhang, Y. Ren, K. Yang, Corros. Sci. 123 (2017) 351–355, https://doi.org/10.1016/j.corsci.2017.04.006.
[6] Y. Fu, X.Q. Wu, E.H. Han, W. Ke, K. Yang, Z.H. Jiang, J. Electrochem. Soc. 155 (2008) C455–C463, https://doi.org/10.1149/1.2939213.
[7] L. Liu, S. Wu, Y. Dong, S. Lü, Corros. Sci. 104 (2016) 236–247, https://doi.org/10.1016/j.corsci.2015.12.016.
[8] Y. Sun, X. Wu, X. Wu, J. Li, Y. Jiang, Int. J. Electrochem. Sci. 11 (2016) 9666–9675, https://doi.org/10.20964/2016.11.28.
[9] E. Ma, T. Zhu, Mater. Today 20 (2017) 323–331, https://doi.org/10.1016/j.mattod.2017.02.003.
[10] K. Lu, J. Lu, Mater. Sci. Eng., A 375–377 (2004) 38–45, https://doi.org/10.1016/j.msea.2003.10.261.
[11] F. Shi, P.C. Tian, N. Jia, Z.H. Ye, Y. Qi, C.M. Liu, X.W. Li, Corros. Sci. 107 (2016) 49–59, https://doi.org/10.1016/j.corsci.2016.02.019.
[12] X.Y. Wang, D.Y. Li, Wear 255 (2003) 836–845, https://doi.org/10.1016/S0043-1648(03)00055-3.
[13] H. Zhang, D. Wang, P. Xue, L.H. Wu, D.R. Ni, B.L. Xiao, Z.Y. Ma, J. Mater. Sci. Technol. 34 (2018) 2183–2188, https://doi.org/10.1016/j.jmst.2018.03.014.
[14] H. Zhang, D. Wang, P. Xue, L.H. Wu, D.R. Ni, Z.Y. Ma, Mater. Des. 110 (2016) 802–810, https://doi.org/10.1016/j.matdes.2016.08.048.
[15] Y. Fu, X. Wu, E.H. Han, W. Ke, K. Yang, Z. Jiang, Electrochim. Acta 54 (2009) 1618–1629, https://doi.org/10.1016/j.electacta.2008.09.053.
[16] B.B. Straumal, Y.O. Kucheev, L.I. Efron, A.L. Petelin, J. Dutta Majumdar, I. Manna, J. Mater. Eng. Perform. 21 (2012) 667–670, https://doi.org/10.1007/s11665-012-0130-6.